Environ. Sci. Technol. **1998**, *32,* 3137−3141

Rate-Limited Transport of Hydroxyatrazine in an Unsaturated Soil

SHELLEY J. KAUFFMAN,*
CARL H. BOLSTER,
GEORGE M. HORNBERGER,
JANET S. HERMAN, AND AARON L. MILLS

University of Virginia, Department of Environmental Sciences, Charlottesville, Virginia 22903

Unsaturated column experiments on an intact soil core were conducted under two different soil pressure heads, -8 and -19 cm, to characterize chemical sorption and desorption for hydroxyatrazine. Breakthrough curves for ^3H_2O were similar under the different experimental conditions. The advection-dispersion transport model described ^3H_2O transport well with Peclet numbers of 0.17 and 0.21, respectively. The transport of hydroxyatrazine, a common degradation product of atrazine, was slightly enhanced at the -8 cm head relative to the -19 cm head (84% vs 79% mass recovery). A model that describes sorption with a single rate coefficient and desorption as a distribution of rate coefficients fits the hydroxyatrazine breakthrough curve well. The strong similarities in transport properties at different soil−water tensions suggests that water and contaminants can be transported through macroporous soils across a range of moisture conditions in the vadose zone in agricultural fields.

Introduction

The extensive movement of agricultural chemicals beyond the root zone generally is attributed to transport through preferred pathways (macropores) created by physical heterogeneities in the soil (*e.g.* cracks, root channels, and worm burrows). In some cases a conceptual model of transport through a macroporous soil with zones of "mobile" water through which water moves, and zones of "immobile" water where water is essentially stagnant, is invoked. In other cases, the classic advection-dispersion model is capable of describing the physical characteristics of transport. Additionally, dissolved contaminants often are affected by rate-limited sorption reactions leading to chemical nonequilibrium. Slow desorption may be important to the overall fate of contaminants by limiting biodegradation (*1*). We investigated how contaminant transport behavior is affected by soil−water tension using an intact soil core obtained from an agricultural clay-silt-loam soil in the Shenandoah Valley of Virginia. The site is actively cultivated with corn and winter wheat. The core used in this study was taken from an area which remains untilled and thus shows evidence of macropore openings in the form of root channels and worm burrows, and a large percentage of the infiltration of this silt-loam soil is attributed to flow in macropores (*2*).

The contaminant used in this study is hydroxyatrazine (HA), an abiotic degradation product of one of the most widely used herbicides, atrazine. Hydroxyatrazine has become ubiquitous in agricultural soils where atrazine is applied and has been found in many groundwater and surface-water systems, despite the fact that it is more sorptive than its parent compound (*3*). Freundlich sorption coefficients for hydroxyatrazine have been observed to be 1 (*3*) to 2 (*4*) orders of magnitude higher than those for atrazine. Hydroxyatrazine is expected to be more persistent than atrazine in soils (*5*), and repeated application of atrazine will likely result in accumulation of hydroxyatrazine in soils (*6*).

Research Approach. We posed a set of questions about hydroxyatrazine transport within the framework of flow through unsaturated soils. (1) Are the kinetics of rate-limited sorption and desorption of hydroxyatrazine affected by the soil−water tension? The sorption of organic compounds in soils typically is described using kinetic expressions. Some have argued that the reactive surfaces on macropore walls should be different from those within the bulk soil (*7*). If so, the kinetics of the sorption and desorption processes may vary with soil−water tension. Few data are available to examine this contention. (2) Must a distribution of sorption sites with different binding energies be employed to describe the sorption and desorption of hydroxyatrazine on soils quantitatively? The sorption process for organic chemicals on soils has been described using single-site models (*8*), a two-site, first-order model (*9*), a two-site spherical diffusion model (*10*), a multireaction model (*11*), and a γ-distributed site model (*12*). The question of whether the γ-distribution model describes transport of hydroxyatrazine and, if so, whether the distribution of sites changes with soil-water content remains open.

Experimental Methods

Intact Columns. An intact soil core (20 cm in diameter, 23 cm long) was taken from the site by driving a stainless steel pipe with a beveled edge into the soil. Because of the claylike nature of the soil, this method proved to be most successful when the soil was at field capacity, when almost no compaction occurred. The steel pipe contained ten 0.3 cm diameter holes randomly distributed for air entry as is necessary for unsaturated transport experiments. The unsaturated column set-up was similar to that of Jardine et al. (*13*), except for the influent flux, which was controlled by a peristaltic pump rather than a Mariotte-bottle device. In the lab the core was fitted on the bottom with an air-tight Teflon housing unit that contained a stainless steel porous plate (40 μm). Acid-washed and DIW-rinsed sand (~0.35 mm) was packed along the uneven bottom edge of the soil to insure direct and complete hydraulic contact with the porous plate. The bottom housing unit of the core was sealed to the top of a vacuum chamber that contained a fraction collector. The tension in the vacuum chamber and subsequently along the bottom boundary of the core was kept constant with a vacuum regulator. The influent solution was added by a peristaltic pump directly to the top of the soil by a Teflon drip chamber with 20 evenly distributed stainless-steel needles, designed to simulate rainfall.

Four soil−water content probes (θ probes, Dynamax, Inc.) were inserted into the core. Two probes were placed on each of two planes, 6 cm from the top and 16 cm from the top of the core, and were programmed to record soil water content every 30 min.

The core was saturated from the bottom with 5 mM solution of NaCl at pH 5.5. This same background solution was then added to the top of the core via the drip chamber at a constant rate, and the appropriate tension was applied

* Corresponding author current address: 160 Park Terrace Ave., West Haven, CT 06516.

S0013-936X(97)01112-7 CCC: $15.00
Published on Web 08/29/1998

to the vacuum chamber at the bottom. Matric heads of -8 and -19 cm were used. At the lower head of -19 cm, the contribution of preferential flow is expected to be smaller. Cores were allowed to stabilize until a steady-state outflow was obtained which typically could be achieved after approximately 5 pore volumes had passed through the soil. Because of the disturbance necessary in removing the core and setting it up, this equilibration time also allowed a "flushing" time for the colloids that were artificially mobilized. The flow rate of the effluent was determined by weighing each fraction of water that was collected for a known increment of time.

Two separate experiments were run on the same core, the first experiment at -19 cm, followed by an experiment at -8 cm (Table 1). These experiments were completed on the same core to allow comparison of the sorption and desorption dynamics without introducing physical variations inherent in different soil cores.

The effluent from the columns was analyzed for colloid-concentration spectrophotometrically at 400 nm wavelength. A standard curve was prepared from colloids eluted from the cores by gravimetrically determining the colloid concentration captured on a 0.1 μm filter.

A solution of 1 mg/L ^{14}C-labeled hydroxyatrazine (0.8 μCi/L) and $^{3}H_2O$ (0.5 μCi/L) in 5 mM NaCl adjusted to pH 5.5 was added as the pulse for all experiments. Both the unfiltered and filtered fractions (0.1 μm) of the effluent were analyzed by liquid scintillation counting. The difference between mass recovery in the unfiltered vs filtered fraction was analyzed to evaluate the potential for colloid-facilitated transport. The effluent also was analyzed for colloid concentration spectrophotometrically.

Model Description

Advection-Dispersion Kinetic Model. Assuming steady-state conditions, the transport of solutes through soil may be described by

$$\frac{\partial c}{\partial t} + \frac{\rho}{\theta}\frac{\partial s}{\partial t} = D\frac{\partial^2 c}{\partial x^2} - v\frac{\partial c}{\partial x} \tag{1}$$

where c is the concentration in the aqueous phase (ML^{-3}), s is the sorbed concentration (MM^{-1}), ρ is the bulk density (ML^{-3}), t is time (T), x is distance (L), θ is the volumetric water content, v is the average pore-water velocity ($L\ T^{-1}$), and D is the dispersion coefficient ($L^2\ T^{-1}$). Following the first-order kinetic reactions of Lapidus and Amundson (*8*), solute retention is described by

$$\frac{\rho}{\theta}\frac{\partial s}{\partial t} = k_f c - k_r\frac{\rho}{\theta}s \tag{2}$$

where k_f and k_r (T^{-1}) are first-order sorption and desorption rate coefficients, respectively.

For convenience of presentation as well as for generalizing the information from the simulations, the model equations were nondimensionalized by defining the following dimensionless variables

$$\kappa_1 = k_f\frac{L}{v} \quad \kappa_2 = k_r\frac{L}{v} \quad S = \frac{s\rho}{C_o\theta}$$

$$T = \frac{vt}{L} \quad X = \frac{x}{L} \quad \mathrm{Pe} = \frac{vL}{D} \quad C = \frac{c}{c_o}$$

where v and L are characteristic velocity and length scales, respectively, c_0 is the concentration in the influent pulse, T is dimensionless time (pore volumes), X is dimensionless length, Pe is the Peclet number, C is reduced aqueous concentration, S is reduced sorbed concentration, and κ_1 and κ_2 are Darnkohler numbers representing time-scale ratios for sorption and desorption to flow velocity, where κ_1 is the sorption coefficient and κ_2 is the desorption coefficient. Given the above dimensionless variables, eqs 1 and 2 become

$$\frac{\partial C}{\partial T} = \frac{1}{\mathrm{Pe}}\frac{\partial^2 C}{\partial X^2} - \frac{\partial C}{\partial X} - \kappa_1 C + \kappa_2 S \tag{3}$$

$$\frac{\partial S}{\partial T} = \kappa_1 C - \kappa_2 S \tag{4}$$

With the small Peclet numbers observed in these experiments, the use of the appropriate boundary conditions becomes critical. For interpreting BTC (breakthrough curve) data, a first-type inlet boundary condition (*14*, *15*) is warranted. Although outlet boundary conditions are more ambiguous, a semi-infinite column is most appropriate for columns of finite length with low Peclet numbers and was approximated by extending the outlet boundary to $X = 8$ (*16*). Initial and boundary conditions for eqs 3 and 4 were

$C = 0$	$X \geq 0$	$T \leq 0$
$S = 0$ (-19 cm)	$X \geq 0$	$T \leq 0$
$S = S_{-19\mathrm{cm}}$(-8 cm)	$X \geq 0$	$T \leq 0$
$C = 1$	$X = 0$	$0 < T < T_0$
$C = 0$	$X = 0$	$T > T_0$
$\frac{\partial C}{\partial X} = 0$	$X = 8$	$T > 0$

For the -8 cm experiment which was run subsequent to the -19 cm experiment the initial sorbed concentration of HA was not equal to zero. To simulate this situation, the calculated residual concentration remaining on the soil surface after the -19 cm experiment was used as the initial sorbed concentration ($S > 0$) in the calculations with the model.

γ-Distributed Desorption Model. The model described above incorporates the assumption that sorption and desorption are controlled by a single kinetic rate parameter. An extension of the model includes multiple sites that vary in mass-transfer rates according to a gamma probability density function (*12*, *17*–*20*). The gamma probability density function (pdf) is given by

$$p(\kappa) = \frac{\beta^{-\eta}\kappa^{\eta-1}}{\Gamma(\eta)}\exp\left(-\frac{\kappa}{\beta}\right) \tag{5}$$

where η is the shape parameter, β is the scale parameter, and Γ is the gamma function. Following Culver et al. (*18*), the continuous pdf is discretized into a finite number of compartments, NK, with each compartment having a distinct kinetic rate coefficient. Each compartment was assumed to occupy an equal fraction of soil. Incorporation of the gamma pdf into the ADE model yields

$$\frac{\partial C}{\partial T} = \frac{1}{\mathrm{Pe}}\frac{\partial^2 C}{\partial X^2} - \frac{\partial C}{\partial X} - \sum_{k=1}^{NK}\left(\frac{\kappa_1}{\mathrm{NK}}C - \kappa_{2_k}\mathrm{S_k}\right) \tag{6}$$

$$\frac{\partial S}{\partial T} = \sum_{k=1}^{\mathrm{NK}}\left(\frac{\kappa_1}{\mathrm{NK}}C - \kappa_{2_k}\mathrm{S_k}\right) \tag{7}$$

where S is the amount sorbed at site k and all other variables are as defined above.

The governing set of equations were solved by the Crank–Nicholson finite-difference method (*21*) using the

TABLE 1. Observed and Calculated Physical and Chemical Parameters for Transport Experiments[a]

	experimental core and applied tension	
	-8 cm	**-19 cm**
	Physical Parameters	
v	0.46	0.37
θ	0.39	0.36
L	20.5	20.5
D	56.6	37.0
pulse	2.5	2.4
Pe	0.17	0.21
E	0.99	0.99
	Dimensionless ADE Kinetic Parameters	
κ_1	5.0	5.7
κ_2	1.3	1.8
E	0.90	0.96
	Dimensional ADE Rate Coefficients	
k_f	0.11	0.10
k_r	0.03	0.03
	Dimensionless γ Kinetic Parameters	
κ_1	6.5	12.1
β	17.0	19.0
η	0.60	0.84
E	0.96	0.98
	Dimensional γ Rate Coefficients	
k_f	0.15	0.21
$k_{r\ (mean)}$	0.22	0.28

[a] For the physical parameters v is the measured average linear pore water velocity (cm/h), θ is the measured volumetric water content, L is the measured column length (cm), pulse is the pulse length in pore volumes, and Pe is the calculated Peclet number. For the single-rate kinetic model κ_1 is the sorption coefficient and κ_2 is the desorption coefficient. For the γ-model β is the scaling parameter, and η is the shape parameter. Dimensional rate coefficients calculated using the definition $\kappa_x = k_x L/v$; k_f = forward rate coefficient (h^{-1}), k_r = backward rate coefficient (h^{-1}).

computer software package MATLAB (Mathworks Inc.). Appropriately simplified forms of the model were verified by comparison with CXTFIT2 (*22*); agreement between the finite-difference approximations and the analytical solutions was excellent.

Results

Column Experiments. The colloids present in the soil water consisted of kaolinite, illite, and particulate organic matter (*4*). During the -8 cm experiment, the average concentration of soil-borne colloids eluted from the column was 110 mg/L, whereas the average concentration eluted during the -19 cm experiment was 10 mg/L. The -19 cm experiment was run before the -8 cm experiment to avoid washing out the colloids for the -8 cm experiment. The observed difference in colloid concentration is most likely due to the different flow rates in the two experiments (Table 1).

Although significant concentrations of colloids were generated, the difference in mass recovery of HA in filtered vs unfiltered fractions was slight. In the -8 cm experiment, only 1% more HA was found in the mass recovered in the unfiltered fraction (84% vs 85%; Figure 1b), and in the -19 cm experiment, only 2% more was found in the unfiltered fraction (79% vs 81%; Figure 2b). Under these experimental conditions hydroxyatrazine transport was not facilitated by soil-borne colloids.

Because the size of the pulse and total volume of water collected was different for the two experiments a closer inspection of the total mass of HA recovered is warranted. Based on an analysis between percent of total mass vs total volume of water passed through the core it is evident that a slightly greater amount of mass is recovered under -8 cm tension (Figure 3).

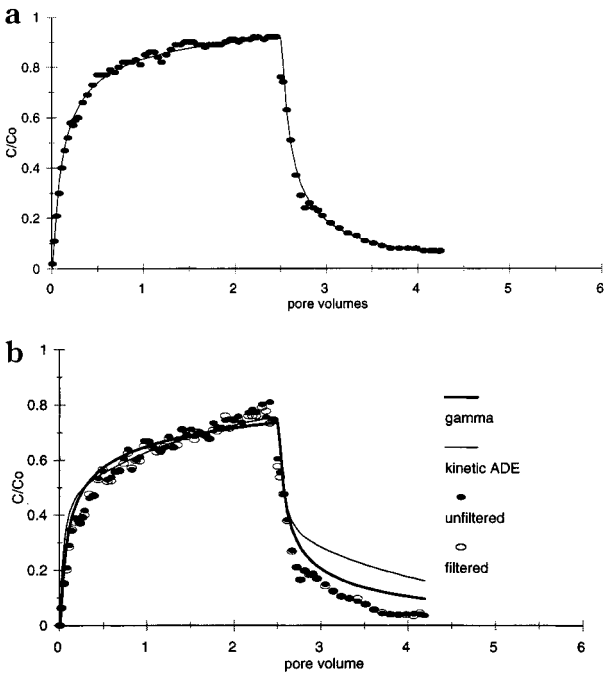

FIGURE 1. (a) Breakthrough curve of ^3H_2O and calculated ADE model fit for -8 cm experiment. (b) Hydroxyatrazine breakthrough (filtered and unfiltered) for -8 cm experiment and calculated curves for the kinetic ADE and γ-distributed desorption (gamma) models.

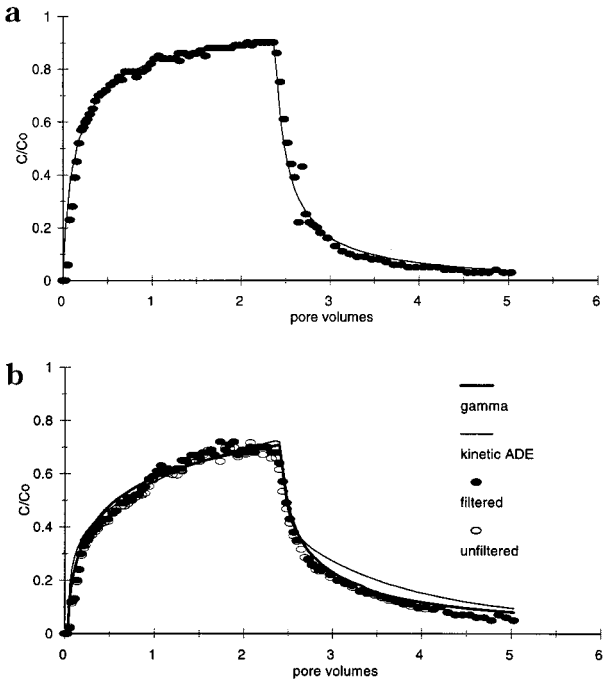

FIGURE 2. (a) Breakthrough curve of ^3H_2O and calculated ADE model fit for -19 cm experiment. (b) Hydroxyatrazine breakthrough (filtered and unfiltered) for -19 cm experiment and calculated curves for the kinetic ADE and γ-distributed desorption (gamma) models.

Breakthrough of ^3H_2O during these experiments shows early arrival indicative of preferential flow through macropores (Figures 1a and 2a). The BTC, however, was described successfully using the advection-dispersion equation (ADE) with a Peclet number of 0.17 for the -8 cm experiment and 0.21 for the -19 cm experiment. These Pe values were then used for describing the hydroxyatrazine BTCs. The mean volumetric water content during these experiments was 0.39 and 0.36 for the -8 and -19 cm experiments, respectively,

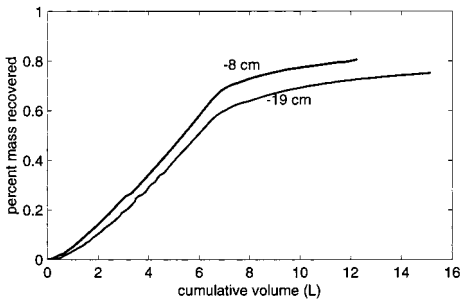

FIGURE 3. Percent total input mass recovered vs cumulative volume passed through the soil core for -8 and -19 cm experiments.

and did not vary more than 5% throughout the each run (Table 1). The lower volumetric water content measured under conditions of a more negative metric potential is evidence that the applied tension did have an affect on the water saturation in the soil.

The arrival of HA was coincident to the arrival of ^3H_2O but at a lower relative concentration indicating kinetic rather than equilibrium sorption. The long tailing of HA is more extensive than can be explained by equilibrium sorption or physical processes. The single-rate kinetic model described the experimental data with a model efficiency (E) (*23*) of 0.90 (-8 cm) and 0.96 (-19 cm).

The HA breakthrough data also were described using the gamma model, and, again, the Pe number determined by the ADE for ^3H_2O was used in the γ-distributed desorption model. For both the -8 and -19 cm experiments, the model that describes desorption with γ-distributed desorption rates provides a far better estimation on the tailing of the hydroxyatrazine breakthrough curve (E = 0.96 and 0.98, respectively) than the ADE kinetic model (Figures 1b and 2b).

Simulations showed that the γ-model was robust for NK, the number of sites used to approximate the continuous distribution, greater than five. For the results presented here, NK was set to 10. The γ-model desorption κ values ranged from 0.10 to 36.7 with a mean of 10.8 although 90% of the κ values fell in a narrower range between 0.10 and 20.8 for the -8 cm experiment. For the -19 cm experiment the κ values ranged from 0.48 to 50.8 with a mean of 15.3, but 90% of the values fell between 0.48 and 31.1. The distributions of κ values under the two experimental tensions were remarkably similar.

With the values for κ_1, and κ_2, that were obtained by best fit of the models, k_f and k_r (the dimensional kinetic sorption coefficients) can be calculated based on the definition $\kappa_x = \kappa_x L/v$ (Table 1). The k_f and k_r values determined by the ADE kinetic model at -19 cm tension are remarkably similar to those at -8 cm tension, whereas the forward rate determined by the gamma model is higher at -19 cm tension.

Discussion

The asymmetrical breakthrough of ^3H_2O is typical of soils exhibiting preferential or macropore flow (*24*). In fact, due to the claylike nature of the soil, the hydraulic conductivity is highly dependent upon preferential flowpaths. This is supported by observations of vastly different hydraulic conductivities for this soil under zero and -15 cm metric head. For example, at saturation mean hydraulic conductivity for this soil is 0.29 cm/min (SD 0.01), and at -15 cm metric head the hydraulic conductivity is greatly reduced to 0.01 cm/min (SD 0.01) (El-Farhan, written communication). The observed BTCs were accurately described with a mobile-immobile model (*22*); however, we chose to use the ADE given the need for fewer fitted parameters. One main concern in using the ADE was the high dispersivity values that were necessary to fit the data. In fact, with either the mobile−immobile model or the ADE, high dispersivity values had to be used to fit the data for both the -8 and -19 cm experiments (27 and 37 cm for mobile−immobile and 100 and 124 cm for ADE, respectively).

The low Peclet numbers observed here are common under conditions of unsaturated flow, especially where the flow regime is heterogeneous (*25*), suggesting that velocity variations within the core are substantial. The higher Peclet number in the -19 cm experiment relative to the -8 cm experiment (Table 1) suggests that less dispersion occurs under the higher tension. A smaller dispersion coefficient indicating smaller flow field velocity variations, which might be expected if less of the flow occurs through preferential flowpaths, has been documented (*13*, *26*). Interestingly, even though velocity variations are substantial (based on high dispersivity values) a single forward-rate coefficient (κ_1), which is inversely proportional to the flow velocity, was capable of describing the sorption of HA in this soil.

The dimensional sorption and desorption coefficients determined by the ADE kinetic model were remarkably similar at the two different soil−water tensions (Table 1). This supports our visual inspection that the BTCs were comparable. Because the sorption rate coefficients are essentially the same for our soil at -8 and -19 cm tension, we infer that contact of the dissolved HA with reactive parts of the soil matrix is the same regardless of soil−water tension (at least at fairly low tensions). Additionally, this suggests that any differences in mass recovery are likely due to diffusion limitations and not kinetic limitations.

Because most of the error in fitting the single-rate kinetic model to the HA breakthrough data arises from an overestimate of the tail of the curve, we chose to describe only desorption as a γ-distributed process. The forward rate coefficient calculated for the gamma model is smaller for the -8 cm experiment relative to the -19 cm experiment, and the mean backward rate coefficient is smaller for the -8 cm experiment, but these differences are not significant because the parameter estimates are not well enough constrained to make that judgment and may in fact be an artifact of the model fit. Note that the tailing limb of the BTC at -8 cm tension is less well represented by the gamma model than the one at -19 cm tension (Figures 1b and 2b). The actual data for the -8 cm case indicated that desorption rates are higher than the model calculations suggest.

Despite the variation noted in both the physical transport parameters and the sorption parameters with soil−water tension, the impact on the overall transport is small indeed. At -8 cm tension, 84% of the applied HA was recovered, and at -19 cm tension, 79% was recovered. Thus, our results indicate that both nonreactive (e.g. ^3H_2O) and strongly sorbing (e.g. HA) solutes are capable of being transported through this soil over a range of soil−water tensions near saturation. Although it appears that larger quantities of dissolved materials are moved per unit of water under conditions of lower tension (Figure 3), the differences are not substantial.

The usefulness of describing desorption as a γ-distribution of site energies has been suggested previously only for historically contaminated and homogeneous soils (*12*, *18*). Culver et al. (*18*) observed a range of four orders of magnitude in the calculated mass-transfer rate coefficients in historically contaminated soils. The implication is that very long contact time allows contaminants to be sorbed to sites that exhibit extraordinarily slow desorption kinetics. The results presented here, however, suggest that the use of a distributed desorption site model may be required to describe desorption even for relatively short contact times. Chen and Wagenet (*17*) recently presented a distributed kinetic site model incorporated into the classic advection-dispersion equation and used it to explain desorption from historically contami-

nated soils. The research presented here extends the usefulness and application of this method to situations where contact times between soil and contaminant are exceedingly short.

Acknowledgments

We thank Teresa Culver for her advice during the development of the gamma model. This research was supported by NSF/EPA Project No. R824772-01-3.

Literature Cited

(1) Harkness, M. R.; McDermott, J. B; Abramowicz, D. A.; Salvo, J. J.; Flanagan, W. P.; Stephens, M. L.; Modello, F. J.; May, R. J.; Lobos, J. H.; Carroll, K. M.; Brennan, M. J.; Bracco, A. A.; Fish, K. M.; Warner, G. L.; Wilson, P. R.; Dietrich, D. K.; Lin, D. T.; Morgan, C. B.; Gately, W. L. *Science* **1993**, *259*, 503−507.
(2) El-Farhan, Y. H.; Waldeck, A. C.; Herman, J. S.; Hornberger, G. M. Abstracts, *EOS*; American Geophysical Union Meeting, San Francisco, CA, 1997.
(3) Clay, S. A.; Koskinen, W. C. *Weed Science* **1990**, *38*, 262−266.
(4) Kauffman, S. J. Ph.D. Dissertation, University of Virginia, 1998.
(5) Lerch, R. N.; Donald, W. W.; Li, X.; Alberts, E. E. *Environ. Sci. Technol.* **1995**, *29*, 2759−2768.
(6) Winkelmann, D. A.; Klaine, S. J. *Environ. Toxicol. Chem.* **1991**, *10*, 335−345.
(7) Stehouwer, R. C.; Dick, W. A.; Traina, S. J. *J. Environ. Qual.* **1993**, *22*, 181−185.
(8) Lapidus, L.; Amundson, N. R. *J. Phys. Chem.* **1952**, *56*, 984−988.
(9) Selim, H. M.; Davidson, J. M.; Mansell, R. S. In *Proceedings of the Summer Computer Simulation Conference*, Washington, DC, 1976.
(10) Brusseau, M. L.; Rao, P. S. C. *Crit. Rev. Environ. Control.* **1989**, *19*, 33−99.
(11) Selim, H. M. *Environ. Health Perspect.* **1989**, *83*, 69−75.
(12) Connaughton, D. F.; Stedinger, J. R.; Lion, L. W.; Shuler, M. L. *Environ. Sci. Technol.* **1993**, *27*, 2397−2403.
(13) Jardine, P. M.; Wilson, G. V.; Jacobs, G. K. *Soil Sci. Soc. Am. J.* **1993**, *57*, 945−953.
(14) Kreft, A.; Zuber, A. *Chem. Eng. Sci.* **1978**, *33*, 1471−1480.
(15) Parker, J. C.; van Genuchten, M. Th. *Water Resour. Res.* **1984**, *20*, 866−872.
(16) Parlange, J.-Y.; Starr, J. L.; van Genuchten, M. Th.; Barry, D. A.; Parker, J. C. *Soil Sci.* **1992**, *153*, 165−171.
(17) Chen, W; Wagenet, R. J. *Soil Sci. Soc. Am. J.* **1997**, *61*, 360−371.
(18) Culver, T. B.; Hallisey, S. P.; Sahoo, D.; Deitsch, J. J.; Smith, J. A. *Environ. Sci. Technol.* **1997**, *31*, 1581−1588.
(19) Pedit, J. A.; Miller, C. T. *Environ. Sci. Technol.* **1994**, *28*, 2094−2104.
(20) Chen, W.; Wagenet, R. J. *Environ. Sci. Technol.* **1995**, *29*, 2725−2734.
(21) Gerald, C. F; Wheatley, P. O. *Applied Numerical Analysis*, 5th ed.; Addison-Wesley: 1994.
(22) Toride, N.; Leij, F. J.; van Genuchten, M. Th. *The CXTFIT code for estimating transport parameters for lab or field tracer experiments: Version 2, Research Report 137*; U. S. Salinity Lab, USDA: Riverside, CA, 1995.
(23) Hornberger, G. M.; Germann, P. F.; Beven, K. J. J. Hydrol. **1991**, 124, 81−99.
(24) Brusseau, M. L.; Jessup, R. E.; Rao, P. S. C. Water Resour. Res. **1989**, 25, 1971−1988.
(25) Beven, K.; Henderson, D. E.; Reeves, A. D. J. Hydrol. **1993**, 143, 19−43.
(26) Seyfried, M. S.; Rao, P. S. C. Soil Sci. Soc. Am. J. **1987**, 51, 1434−1444.

Received for review December 22, 1997. Revised manuscript received April 20, 1998. Accepted July 2, 1998.

ES9711122